First observation of the decays $\chi_{cJ} \to \pi^0\pi^0\pi^0\pi^0$

M. Ablikim,[1] M. N. Achasov,[5] L. An,[9] Q. An,[36] Z. H. An,[1] J. Z. Bai,[1] R. Baldini,[17] Y. Ban,[23] J. Becker,[2] N. Berger,[1] M. Bertani,[17] J. M. Bian,[1] I. Boyko,[15] R. A. Briere,[3] V. Bytev,[15] X. Cai,[1] G. F. Cao,[1] X. X. Cao,[1] J. F. Chang,[1] G. Chelkov,[15,*] G. Chen,[1] H. S. Chen,[1] J. C. Chen,[1] M. L. Chen,[1] S. J. Chen,[21] Y. Chen,[1] Y. B. Chen,[1] H. P. Cheng,[11] Y. P. Chu,[1] D. Cronin-Hennessy,[35] H. L. Dai,[1] J. P. Dai,[1] D. Dedovich,[15] Z. Y. Deng,[1] I. Denysenko,[15,†] M. Destefanis,[38] Y. Ding,[19] L. Y. Dong,[1] M. Y. Dong,[1] S. X. Du,[42] M. Y. Duan,[26] R. R. Fan,[1] J. Fang,[1] S. S. Fang,[1] F. Feldbauer,[2] C. Q. Feng,[36] C. D. Fu,[1] J. L. Fu,[21] Y. Gao,[32] C. Geng,[36] K. Goetzen,[7] W. X. Gong,[1] M. Greco,[38] S. Grishin,[15] M. H. Gu,[1] Y. T. Gu,[9] Y. H. Guan,[6] A. Q. Guo,[22] L. B. Guo,[20] Y. P. Guo,[22] X. Q. Hao,[1] F. A. Harris,[34] K. L. He,[1] M. He,[1] Z. Y. He,[22] Y. K. Heng,[1] Z. L. Hou,[1] H. M. Hu,[1] J. F. Hu,[6] T. Hu,[1] B. Huang,[1] G. M. Huang,[12] J. S. Huang,[10] X. T. Huang,[25] Y. P. Huang,[1] T. Hussain,[37] C. S. Ji,[36] Q. Ji,[1] X. B. Ji,[1] X. L. Ji,[1] L. K. Jia,[1] L. L. Jiang,[1] X. S. Jiang,[1] J. B. Jiao,[25] Z. Jiao,[11] D. P. Jin,[1] S. Jin,[1] F. F. Jing,[32] M. Kavatsyuk,[16] S. Komamiya,[31] W. Kuehn,[33] J. S. Lange,[33] J. K. C. Leung,[30] Cheng Li,[36] Cui Li,[36] D. M. Li,[42] F. Li,[1] G. Li,[1] H. B. Li,[1] J. C. Li,[1] Lei Li,[1] N. B. Li,[20] Q. J. Li,[1] W. D. Li,[1] W. G. Li,[1] X. L. Li,[25] X. N. Li,[1] X. Q. Li,[22] X. R. Li,[1] Z. B. Li,[28] H. Liang,[36] Y. F. Liang,[27] Y. T. Liang,[33] G. R. Liao,[8] X. T. Liao,[1] B. J. Liu,[29] B. J. Liu,[30] C. L. Liu,[3] C. X. Liu,[1] C. Y. Liu,[1] F. H. Liu,[26] Fang Liu,[1] Feng Liu,[12] G. C. Liu,[1] H. Liu,[1] H. B. Liu,[6] H. M. Liu,[1] H. W. Liu,[1] J. P. Liu,[40] K. Liu,[23] K. Y. Liu,[19] Q. Liu,[34] S. B. Liu,[36] X. Liu,[18] X. H. Liu,[1] Y. B. Liu,[22] Y. W. Liu,[36] Yong Liu,[1] Z. A. Liu,[1] Z. Q. Liu,[1] H. Loehner,[16] G. R. Lu,[10] H. J. Lu,[11] J. G. Lu,[1] Q. W. Lu,[26] X. R. Lu,[6] Y. P. Lu,[1] C. L. Luo,[20] M. X. Luo,[41] T. Luo,[1] X. L. Luo,[1] C. L. Ma,[6] F. C. Ma,[19] H. L. Ma,[1] Q. M. Ma,[1] T. Ma,[1] X. Ma,[1] X. Y. Ma,[1] M. Maggiora,[38] Q. A. Malik,[37] H. Mao,[1] Y. J. Mao,[23] Z. P. Mao,[1] J. G. Messchendorp,[16] J. Min,[1] R. E. Mitchell,[14] X. H. Mo,[1] C. Motzko,[2] N. Yu. Muchnoi,[5] Y. Nefedov,[15] Z. Ning,[1] S. L. Olsen,[24] Q. Ouyang,[1] S. Pacetti,[17] M. Pelizaeus,[34] K. Peters,[7] J. L. Ping,[20] R. G. Ping,[1] R. Poling,[35] C. S. J. Pun,[30] M. Qi,[21] S. Qian,[1] C. F. Qiao,[6] X. S. Qin,[1] J. F. Qiu,[1] K. H. Rashid,[37] G. Rong,[1] X. D. Ruan,[9] A. Sarantsev,[15,‡] J. Schulze,[2] M. Shao,[36] C. P. Shen,[34] X. Y. Shen,[1] H. Y. Sheng,[1] M. R. Shepherd,[14] X. Y. Song,[1] S. Sonoda,[31] S. Spataro,[38] B. Spruck,[33] D. H. Sun,[1] G. X. Sun,[1] J. F. Sun,[10] S. S. Sun,[1] X. D. Sun,[1] Y. J. Sun,[36] Y. Z. Sun,[1] Z. J. Sun,[1] Z. T. Sun,[36] C. J. Tang,[27] X. Tang,[1] X. F. Tang,[8] H. L. Tian,[1] D. Toth,[35] G. S. Varner,[34] X. Wan,[1] B. Q. Wang,[23] K. Wang,[1] L. L. Wang,[4] L. S. Wang,[1] M. Wang,[25] P. Wang,[1] P. L. Wang,[1] Q. Wang,[1] S. G. Wang,[23] X. L. Wang,[36] Y. D. Wang,[36] Y. F. Wang,[1] Y. Q. Wang,[25] Z. Wang,[1] Z. G. Wang,[1] Z. Y. Wang,[1] D. H. Wei,[8] S. P. Wen,[1] U. Wiedner,[2] L. H. Wu,[1] N. Wu,[1] W. Wu,[19] Z. Wu,[1] Z. J. Xiao,[20] Y. G. Xie,[1] G. F. Xu,[1] G. M. Xu,[23] H. Xu,[1] Y. Xu,[22] Z. R. Xu,[36] Z. Z. Xu,[36] Z. Xue,[1] L. Yan,[36] W. B. Yan,[36] Y. H. Yan,[13] H. X. Yang,[1] M. Yang,[1] T. Yang,[9] Y. Yang,[12] Y. X. Yang,[8] M. Ye,[1] M. H. Ye,[4] B. X. Yu,[1] C. X. Yu,[22] L. Yu,[12] C. Z. Yuan,[1] W. L. Yuan,[20] Y. Yuan,[1] A. A. Zafar,[37] A. Zallo,[17] Y. Zeng,[13] B. X. Zhang,[1] B. Y. Zhang,[1] C. C. Zhang,[1] D. H. Zhang,[1] H. H. Zhang,[28] H. Y. Zhang,[1] J. Zhang,[20] J. W. Zhang,[1] J. Y. Zhang,[1] J. Z. Zhang,[1] L. Zhang,[21] S. H. Zhang,[1] T. R. Zhang,[20] X. J. Zhang,[1] X. Y. Zhang,[25] Y. Zhang,[1] Y. H. Zhang,[1] Z. P. Zhang,[36] Z. Y. Zhang,[40] G. Zhao,[1] H. S. Zhao,[1] Jiawei Zhao,[36] Jingwei Zhao,[1] Lei Zhao,[36] Ling Zhao,[1] M. G. Zhao,[22] Q. Zhao,[1] S. J. Zhao,[42] T. C. Zhao,[39] X. H. Zhao,[21] Y. B. Zhao,[1] Z. G. Zhao,[36] Z. L. Zhao,[9] A. Zhemchugov,[15,*] B. Zheng,[1] J. P. Zheng,[1] Y. H. Zheng,[6] Z. P. Zheng,[1] B. Zhong,[1] J. Zhong,[2] L. Zhong,[32] L. Zhou,[1] X. K. Zhou,[6] X. R. Zhou,[36] C. Zhu,[1] K. Zhu,[1] K. J. Zhu,[1] S. H. Zhu,[1] X. L. Zhu,[32] X. W. Zhu,[1] Y. S. Zhu,[1] Z. A. Zhu,[1] J. Zhuang,[1] B. S. Zou,[1] J. H. Zou,[1] J. X. Zuo,[1] and P. Zweber[35]

(BESIII Collaboration)

[1]*Institute of High Energy Physics, Beijing 100049, People's Republic of China*
[2]*Bochum Ruhr-University, 44780 Bochum, Germany*
[3]*Carnegie Mellon University, Pittsburgh, Pennsylvania 15213, USA*
[4]*China Center of Advanced Science and Technology, Beijing 100190, People's Republic of China*
[5]*G.I. Budker Institute of Nuclear Physics SB RAS (BINP), Novosibirsk 630090, Russia*
[6]*Graduate University of Chinese Academy of Sciences, Beijing 100049, People's Republic of China*
[7]*GSI Helmholtzcentre for Heavy Ion Research GmbH, D-64291 Darmstadt, Germany*
[8]*Guangxi Normal University, Guilin 541004, People's Republic of China*
[9]*Guangxi University, Naning 530004, People's Republic of China*
[10]*Henan Normal University, Xinxiang 453007, People's Republic of China*
[11]*Huangshan College, Huangshan 245000, People's Republic of China*
[12]*Huazhong Normal University, Wuhan 430079, People's Republic of China*
[13]*Hunan University, Changsha 410082, People's Republic of China*
[14]*Indiana University, Bloomington, Indiana 47405, USA*
[15]*Joint Institute for Nuclear Research, 141980 Dubna, Russia*

[16]*KVI/University of Groningen, 9747 AA Groningen, The Netherlands*
[17]*Laboratori Nazionali di Frascati - INFN, 00044 Frascati, Italy*
[18]*Lanzhou University, Lanzhou 730000, People's Republic of China*
[19]*Liaoning University, Shenyang 110036, People's Republic of China*
[20]*Nanjing Normal University, Nanjing 210046, People's Republic of China*
[21]*Nanjing University, Nanjing 210093, People's Republic of China*
[22]*Nankai University, Tianjin 300071, People's Republic of China*
[23]*Peking University, Beijing 100871, People's Republic of China*
[24]*Seoul National University, Seoul, 151-747 Korea*
[25]*Shandong University, Jinan 250100, People's Republic of China*
[26]*Shanxi University, Taiyuan 030006, People's Republic of China*
[27]*Sichuan University, Chengdu 610064, People's Republic of China*
[28]*Sun Yat-Sen University, Guangzhou 510275, People's Republic of China*
[29]*The Chinese University of Hong Kong, Shatin, N.T., Hong Kong*
[30]*The University of Hong Kong, Pokfulam, Hong Kong*
[31]*The University of Tokyo, Tokyo 113-0033 Japan*
[32]*Tsinghua University, Beijing 100084, People's Republic of China*
[33]*Universitaet Giessen, 35392 Giessen, Germany*
[34]*University of Hawaii, Honolulu, Hawaii 96822, USA*
[35]*University of Minnesota, Minneapolis, Minnesota 55455, USA*
[36]*University of Science and Technology of China, Hefei 230026, People's Republic of China*
[37]*University of the Punjab, Lahore-54590, Pakistan*
[38]*University of Turin and INFN, Turin, Italy*
[39]*University of Washington, Seattle, Washington 98195, USA*
[40]*Wuhan University, Wuhan 430072, People's Republic of China*
[41]*Zhejiang University, Hangzhou 310027, People's Republic of China*
[42]*Zhengzhou University, Zhengzhou 450001, People's Republic of China*

We present a study of the P-wave spin-triplet charmonium χ_{cJ} decays ($J = 0, 1, 2$) into $\pi^0\pi^0\pi^0\pi^0$. The analysis is based on 106×10^6 ψ' decays recorded with the BESIII detector at the BEPCII electron positron collider. The decay into the $\pi^0\pi^0\pi^0\pi^0$ hadronic final state is observed for the first time. We measure the branching fractions $B(\chi_{c0} \to \pi^0\pi^0\pi^0\pi^0) = (3.34 \pm 0.06 \pm 0.44) \times 10^{-3}$, $B(\chi_{c1} \to \pi^0\pi^0\pi^0\pi^0) = (0.57 \pm 0.03 \pm 0.08) \times 10^{-3}$, and $B(\chi_{c2} \to \pi^0\pi^0\pi^0\pi^0) = (1.21 \pm 0.05 \pm 0.16) \times 10^{-3}$, where the uncertainties are statistical and systematical, respectively.

I. INTRODUCTION

In the quark model, the χ_{cJ} ($J = 0, 1, 2$) mesons are the $3P_J$ charmonium states. Their decays are experimentally and theoretically not as well studied as the vector charmonium states J/ψ and ψ'. In contrast to the latter ones, χ_{cJ} cannot be produced directly in e^+e^- annihilation. However, they can be produced in radiative decays $\psi' \to \gamma\chi_{cJ}$, providing a clean environment to study their decays.

Recent theoretical work indicates that the color octet mechanism [1] could have large contributions to the decays of the P-wave charmonium states. However, these calculations, as well as experimental measurements, still have large errors and thus more precise experimental data besides more theoretical efforts are mandatory to further understand χ_{cJ}

decay dynamics. Furthermore, the χ_{c0} and χ_{c2} states are expected to annihilate via two-gluon processes into light hadrons and may therefore allow the study of glueball dynamics. Thus, the measurement of as many exclusive hadronic χ_{cJ} decays as possible is valuable.

The χ_{cJ} decays into four pions have the largest branching fractions among the known hadronic χ_{cJ} decay modes [2]. Currently only the decays into $\pi^+\pi^-\pi^+\pi^-$ and into $\pi^+\pi^-\pi^0\pi^0$ are measured by previous experiments. The branching fractions are shown in Table I. In this paper, we present a study of exclusive χ_{cJ} decays into $\pi^0\pi^0\pi^0\pi^0$.

II. THE BESIII EXPERIMENT AND DATA SET

We use a data sample of about 106×10^6 ψ' decays recorded with the BESIII detector [3] at the energy-symmetric double-ring e^+e^- collider BEPCII [4]. The primary data sample corresponds to an integrated luminosity of 156.4 pb^{-1} collected at the peak of the ψ' resonance. In addition, a 42.6 pb^{-1} data sample collected about 36 MeV below the resonance is used for background studies.

---
*Also at the Moscow Institute of Physics and Technology, Moscow, Russia.
†On leave from the Bogolyubov Institute for Theoretical Physics, Kiev, Ukraine.
‡Also at the PNPI, Gatchina, Russia.

TABLE I. Branching fractions of χ_{cJ} into $\pi^+ \pi^- \pi^+ \pi^-$ and $\pi^+ \pi^- \pi^0 \pi^0$ [2].

Channel	Branching fraction [%]
$\chi_{c0} \rightarrow \pi^+ \pi^- \pi^+ \pi^-$	2.27 ± 0.19
$\chi_{c1} \rightarrow \pi^+ \pi^- \pi^+ \pi^-$	0.76 ± 0.26
$\chi_{c2} \rightarrow \pi^+ \pi^- \pi^+ \pi^-$	1.11 ± 0.11
$\chi_{c0} \rightarrow \pi^+ \pi^- \pi^0 \pi^0$	3.4 ± 0.4
$\chi_{c1} \rightarrow \pi^+ \pi^- \pi^0 \pi^0$	1.26 ± 0.17
$\chi_{c2} \rightarrow \pi^+ \pi^- \pi^0 \pi^0$	2.00 ± 0.26

The BESIII detector is described in detail elsewhere [3]. Charged particle momenta are measured with a small-celled, helium gas-based main drift chamber with 43 layers operating within the 1 T magnetic field of a solenoidal superconducting magnet. Charged particle identification is provided by measurements of the specific ionization energy loss dE/dx in the tracking device and by means of a plastic scintillator time of flight system composed of a barrel part and two end caps. Photons are detected and their energies and positions measured with an electromagnetic calorimeter (EMC) consisting of 6240 CsI(Tl) crystals arranged in a barrel and two end caps. The return yoke of the magnet is instrumented with resistive plate chambers arranged in 9 (barrel) and 8 layers (end caps) for the discrimination of muons and charged hadrons.

III. DATA SELECTION

We reconstruct the entire event from the decay chain of the charmonium transitions $\psi' \rightarrow \gamma \chi_{cJ}$ followed by the hadronic decays $\chi_{cJ} \rightarrow \pi^0 \pi^0 \pi^0 \pi^0$. A photon candidate is defined as a shower detected with the EMC exceeding an energy deposit of 25 MeV in the barrel region (covering the region $|\cos\theta| < 0.8$ of the polar angle) and of 50 MeV in the end caps ($0.86 < |\cos\theta| < 0.92$). The average event vertex of each run is assumed as the origin of these candidates. We restrict the analysis to events having nine photon candidates and no reconstructed charged particle. The energy sum of the nine photons must be within the range 3.45–3.80 GeV. To reconstruct $\pi^0 \rightarrow \gamma\gamma$ candidates we use pairs of photon candidates, having an invariant mass between 110 and 150 MeV/c^2. Figure 1 shows the invariant $\gamma\gamma$ mass distribution of all photon pair combinations for selected 9γ events. A clear π^0 signal is visible. By combining four π^0 candidates with an additional photon candidate being detected in the EMC barrel, where the same photon candidate must not be used more than once, the complete event is reconstructed. Different pairings of the photon candidates can yield more than one $\gamma \pi^0 \pi^0 \pi^0 \pi^0$ candidate per event. Therefore, we use the pairing which leads to the minimal

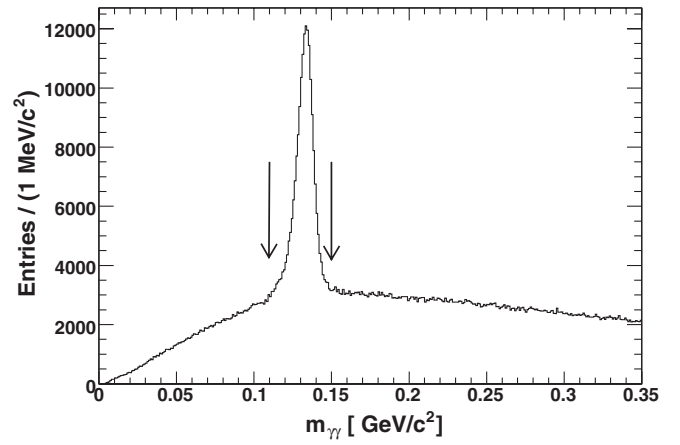$$\chi^2_{4\pi} = \sum_i \frac{(m_{\gamma\gamma,i} - m_{\pi^0})^2}{\sigma^2} \tag{1}$$

FIG. 1. Invariant $\gamma\gamma$ mass distribution of all photon pair combinations for selected 9γ events. The arrows indicate the mass window used for the selection of π^0 candidates.

calculated from the invariant mass $m_{\gamma\gamma,i}$ of the i-th π^0 candidate for a given $\gamma\pi^0\pi^0\pi^0\pi^0$ candidate, the nominal π^0 mass [2] m_{π^0}, and the $\pi^0 \rightarrow \gamma\gamma$ invariant mass resolution σ of 6.5 MeV/c^2. Combinatorial background is suppressed strongly by demanding $\chi^2_{4\pi} < 15$.

Potential backgrounds can arise from the transition $\psi' \rightarrow \pi^0 \pi^0 J/\psi$ followed by hadronic or radiative decays of the J/ψ to final states with higher photon multiplicity. We therefore require the recoil mass m_R of any di-π^0 pair with respect to the ψ' to be $|m_R - m_{J/\psi}| > 100$ MeV/c^2, where $m_{J/\psi}$ is the nominal J/ψ mass [2].

The spectrum of the energy E^*_γ of the photon from the ψ' radiative transition in the center of mass frame is shown in Fig. 2. Clear χ_{c0}, χ_{c1}, and χ_{c2} signals with small background are evident. An analysis of the continuum data sample yields only four events passing the selection criteria

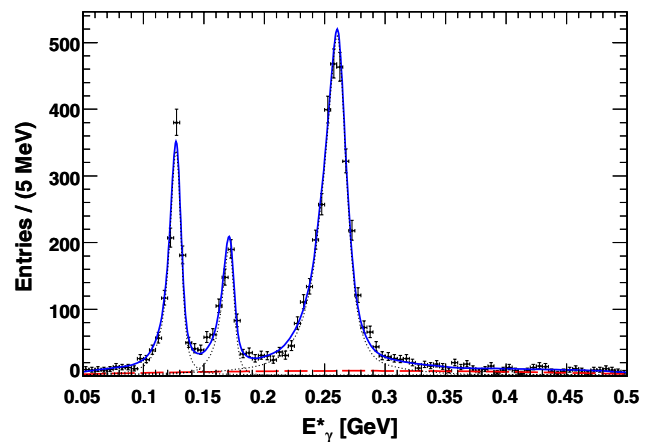FIG. 2 (color online). The spectrum of the energy E^*_γ of the radiative photon from $\psi' \rightarrow \gamma \chi_{cJ}$ with the result of the fit (solid curve) described in the text. The dashed curve shows the background line shape and the dotted curves represent the signal line shapes derived from MC simulations (see Sec. V).
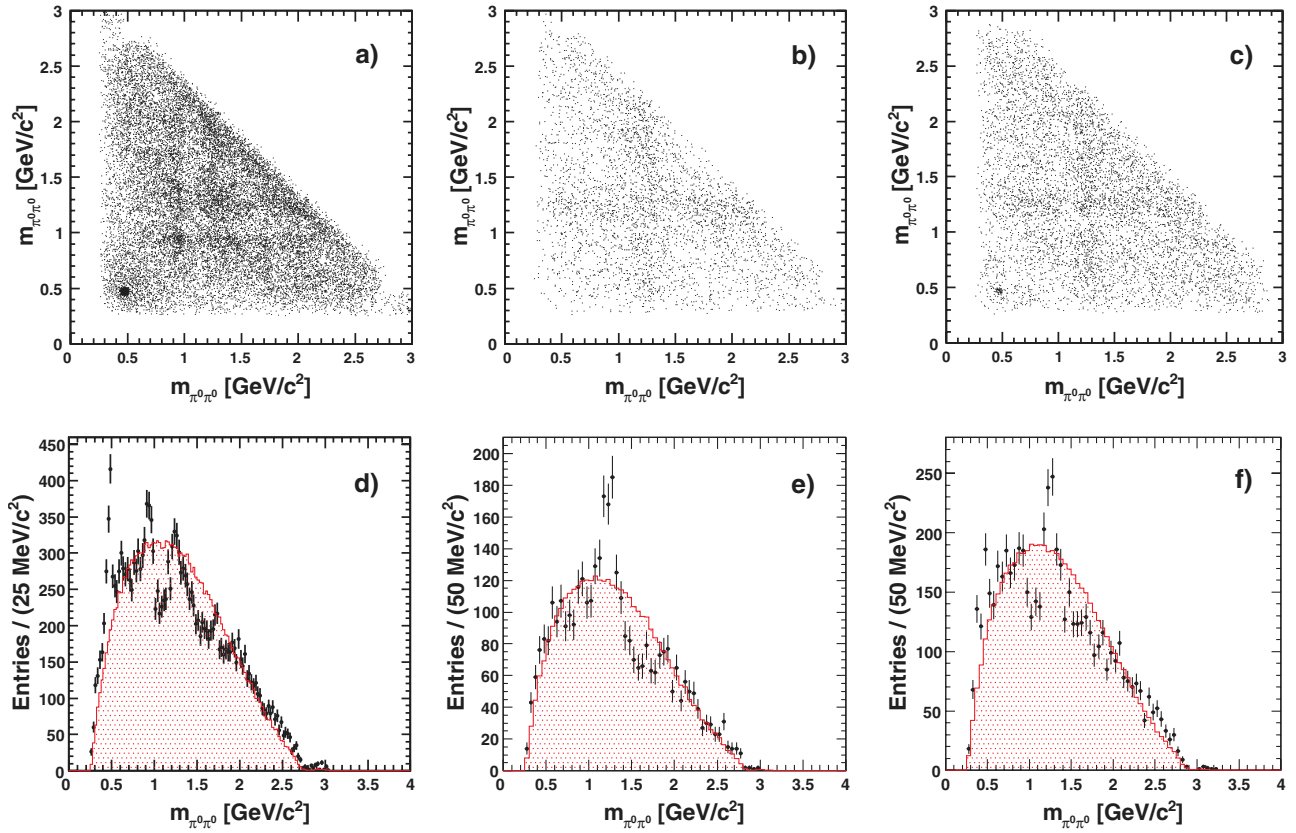
FIG. 3 (color online). Shown is the invariant di-π^0 mass plotted versus the other invariant di-π^0 mass for events selected from the (a) χ_{c0}, (b) χ_{c1}, and (c) χ_{c2} signal regions. All possible $\pi^0\pi^0$ combinations of the $\pi^0\pi^0\pi^0\pi^0$ hadronic final state are plotted. In addition the plots are symmetrized; thus, each event enters 6 times to the plots. The one-dimensional projections are shown in (d), (e), and (f) for χ_{c0}, χ_{c1}, and χ_{c2}, respectively, where the dots with error bars show the data and the shaded histograms show the di-π^0 mass distributions obtained from signal MC events simulated without intermediate resonances for the χ_{cJ} decays.

and thus reveals no significant background. Peaking components of the background are investigated from simulated Monte Carlo (MC) events and are discussed in Sec. IV.

We further look into resonant substructures in the $\pi^0\pi^0\pi^0\pi^0$ final state. The production of intermediate resonances in the decay could have an impact on the detection efficiencies. Here, we only investigate the gross substructures by plotting the invariant mass of any di-π^0 pair in the final state versus the corresponding mass of the other pair for the three χ_{cJ} signal regions (Fig. 3). The defined χ_{c0}, χ_{c1}, and χ_{c2} signal regions correspond to E_γ^* energy ranges of 220–290 MeV, 160–180 MeV, and 115–135 MeV, respectively. As seen in Fig. 3, production of K_S^0 and $f_0(980)$ in the χ_{c0} decay is evident. The accumulation of events is also observed in the mass region around 1300, 1700, and 1950 MeV/c^2. Structures around 1300 MeV/c^2 are observed in χ_{c1} and χ_{c2} decays. All these structures need further careful investigation using partial wave analysis techniques with increased data samples being collected in the future. As for χ_{c0} decays, K_S^0 production is also observed in χ_{c2} decays, while the decay $\chi_{c1} \to K_S^0 K_S^0$ is forbidden by parity conservation.

For the measurement of branching fractions we include all subresonant decay modes but explicitly exclude the χ_{c0} and χ_{c2} decay mode to $K_S^0 K_S^0$. Therefore, we reject events where the invariant mass m_{12} of any di-π^0 pair and the invariant mass m_{34} of the corresponding other di-π^0 pair of the $\gamma\pi^0\pi^0\pi^0\pi^0$ final state fulfills

$$\sqrt{(m_{12} - m_{K_S^0})^2 + (m_{34} - m_{K_S^0})^2} < 100 \text{ MeV}/c^2, \quad \text{where}$$

$m_{K_S^0}$ is the nominal K_S^0 mass [2].

IV. MONTE CARLO STUDIES

A detailed MC simulation of the BESIII detector based on GEANT4 [5] is used to determine efficiencies, signal shapes, and background contributions. The production of the ψ' resonance is simulated using the KKMC event generator [6]. Decays of the ψ' and subsequent particles in the event are modeled by EVTGEN [7]. Simulated events pass the same reconstruction algorithms and selection criteria as data.

Signal MC data samples of 500 k events for each decay $\psi' \to \gamma\chi_{cJ}$, $\chi_{cJ} \to \pi^0\pi^0\pi^0\pi^0$ are generated using a $1 + \lambda\cos^2(\theta)$ distribution, where θ is the angle between the

TABLE II.   Expected number of background events peaking at the χ_{cJ} signal regions as derived from MC simulations.

Channel	$n_{\chi_{c0}}$	$n_{\chi_{c1}}$	$n_{\chi_{c2}}$
$\chi_{c0} \to K_S^0 K_S^0,\ K_S^0 \to \pi^0\pi^0$	1.6	0.3	0
$\chi_{c0} \to \eta\eta$	0.2	0	0
$\chi_{c1} \to \eta\pi^0\pi^0$	1.2	45.2	0
$\chi_{c1} \to \gamma J/\psi,\ J/\psi \to \omega\pi^0\pi^0$	0	1.3	0
$\chi_{c1} \to \gamma J/\psi,\ J/\psi \to \eta\pi^0\pi^0$	0	0	0.1
$\chi_{c2} \to K_S^0 K_S^0,\ K_S^0 \to \pi^0\pi^0$	0	0	0.6
$\chi_{c2} \to \eta\pi^0\pi^0$	0	0	3.8
$\chi_{c2} \to \eta\eta$	0	0	0
$\chi_{c2} \to \gamma J/\psi,\ J/\psi \to \omega\pi^0\pi^0$	0	0	0.6
$\chi_{c2} \to \gamma J/\psi,\ J/\psi \to \eta\pi^0\pi^0$	0	0	0
Sum	3.0	46.8	5.1

direction of the radiative photon and the positron beam, and $\lambda = 1,\ -1/3,\ 1/13$ for $J = 0,\ 1,\ 2$ in accord with expectations for electric dipole (E1) transitions. The χ_{cJ} decay products are generated using a flat angular distribution. Intrinsic width and mass values as given in [2] are used for the χ_{cJ} states in the simulation. The obtained efficiencies for χ_{c0}, χ_{c1}, and χ_{c2} are $(10.16 \pm 0.05)\%$, $(11.54 \pm 0.05)\%$, and $(10.85 \pm 0.05)\%$, respectively, including detector acceptance as well as reconstruction and selection efficiencies.

In addition we use MC data samples to investigate sources of the peaking backgrounds. For each of the studied χ_{cJ} decay modes listed in Table II we generated at least 100 k events. The contribution of the total peaking background is estimated from a fit to the reconstructed E_γ^* spectrum. The fit procedure is the same as applied for data and will be addressed in Sec. V. The largest peaking background contribution is found to come from $\chi_{c1} \to \eta\pi^0\pi^0$ decays, with $\eta \to \pi^0\pi^0\pi^0$, where one of the π^0 has low momentum and is not detected.

V. FITTING PROCEDURE AND EXTRACTION OF BRANCHING FRACTIONS

The E_γ^* spectrum shown in Fig. 2 is fitted using an unbinned maximum likelihood fit. The χ_{cJ} signal line shapes are extracted from the MC simulation. A 2nd order Chebychev polynomial is used to describe the nonpeaking background. From the fit χ_{c0}, χ_{c1}, and χ_{c2} signal yields of 3299 ± 67, 655 ± 32, and 1169 ± 41, respectively, are obtained.

To access the goodness of the fit, we repeat the fit to the E_γ^* spectrum using a binned least-squared fit. Applying a binning of 5 MeV, this fit yields a χ^2 value of 102 with 84 degrees of freedom.

The fit does not account for the peaking component of the background. We estimate the number of events peaking at the position of the χ_{cJ} signals by fitting the E_γ^* spectrum derived from the MC samples generated for background

studies. The same fitting procedure as for data is applied, except that the parameters of the polynomial function describing the shape of the nonpeaking combinatorial background are fixed to the values obtained from the fit to data. From the extracted signal yields the expected number of peaking background events is calculated using the branching fractions of the χ_{cJ} decays as given in [2]. We relate the unmeasured branching fractions of the decays $\chi_{cJ} \to \eta\pi^0\pi^0$ to the corresponding branching fractions of $\chi_{cJ} \to \eta\pi^+\pi^-$ decays by the isospin ratio of the two final states. The estimated number of peaking background events for the investigated channels is given in Table II. In total a peaking background of 3.0, 46.8 and 5.1 events to the χ_{c0}, χ_{c1}, and χ_{c2} signals, respectively, are derived. The largest contribution arises from the decay $\chi_{c1} \to \eta\pi^0\pi^0$, amounting to 45 events at the χ_{c1} signal region.

Although $\chi_{c0} \to K_S^0 K_S^0$ and $\chi_{c2} \to K_S^0 K_S^0$ decays for the branching fraction measurement were excluded, we considered these channels as a potential peaking background source. The feedthrough of the two decays to the χ_{c0}, χ_{c1}, and χ_{c2} signals is expected to be 1.6, 0.3, and 0.6 events, respectively.

The expected number of peaking background events is subtracted from the yields observed for data. These corrected yields N are then converted to branching fractions using

$$\mathcal{B}(\chi_{cJ} \to 4\pi^0) = \frac{N}{\epsilon \cdot N_{\psi'} \cdot \mathcal{B}(\psi' \to \gamma\chi_{cJ}) \cdot \mathcal{B}(\pi^0 \to \gamma\gamma)^4},$$
(2)

where ϵ is the efficiency; $N\psi'$ is the number of ψ' in the data sample; and $\mathcal{B}(\psi' \to \gamma\chi_{cJ})$ and $\mathcal{B}(\pi^0 \to \gamma\gamma)$ are the branching fractions of radiative ψ' transitions into χ_{cJ} and of the decay $\pi^0 \to \gamma\gamma$ [2], respectively. The number of ψ' and its combined statistical and systematical uncertainties are determined to be $N_{\psi'} = (1.06 \pm 0.04) \times 10^8$ [8].

VI. ESTIMATION OF SYSTEMATIC UNCERTAINTIES

Several sources of systematic uncertainties are considered for the measurement of the branching fractions, including uncertainties on the photon detection and reconstruction; the event selection; the fitting procedure and peaking background subtraction; and the number of ψ' decays in the data sample. The investigated uncertainties are summarized in Table III and will be discussed in detail in the following.

(a) *Photon detection*—The uncertainty due to photon detection and conversion is 1% per photon. This is determined from studies of photon detection in well-understood decays such as $J/\psi \to \rho^0\pi^0$ and the study of photon conversion in the process $e^+e^- \to \gamma\gamma$.

TABLE III.   Summary of the systematic uncertainties.

	χ_{c0}[%]	χ_{c1}[%]	χ_{c2}[%]
Photon detection	9.0	9.0	9.0
Decay model	6.3	6.3	6.3
$\mathcal{B}(\psi' \to \gamma\chi_{cJ})$	3.2	4.3	4.0
Number of ψ' events	4.0	4.0	4.0
Total energy	3.0	3.0	3.0
$\chi^2_{4\pi}$	2.5	2.5	2.5
Reconstructed π^0 mass	1.4	1.4	1.4
Fitting range	1.4	2.9	0.9
Signal line shape (energy resolution)	0.5	1.2	0.4
Signal line shape (energy shift)	0.1	0.6	1.0
Background shape	1.0	1.0	1.0
Peaking background subtraction	0.1	0.8	0.5
MC statistics	0.5	0.5	0.5
Trigger efficiency	<0.1	<0.1	<0.1
Total uncertainty	13.2	13.6	13.2

(b) Event selection—By varying the requirement on $\chi^2_{4\pi}$, the π^0 mass window and the total energy of the $\gamma\pi^0\pi^0\pi^0\pi^0$ candidates used for the event selection in data and MC events, we investigate the systematic uncertainties in modeling the distribution of these parameters. The largest deviation of the branching fractions from the default values sets the scale of our systematic uncertainty, and we assign an uncertainty of 2.5% for the $\chi^2_{4\pi}$, 3% for the total energy, and 1.4% for the π^0 mass window requirement.

(c) Monte Carlo decay model—The efficiencies for the processes $\psi' \to \gamma\chi_{cJ}$, $\chi_{cJ} \to \pi^0\pi^0\pi^0\pi^0$ are determined from MC simulations, where no intermediate resonances and a flat angular distribution have been considered in the χ_{cJ} decays. As discussed in Sec. III this analysis reveals the presence of intermediate resonances in the $\chi_{cJ} \to \pi^0\pi^0\pi^0\pi^0$ decays. This could have an impact on the detection efficiencies, which we consider as a systematic uncertainty. We determine the efficiencies from our simulations including the subresonant modes $f_0(980)f_0(980)$, $f_2(1270)f_2(1270)$, $f_0(1370)f_0(1500)$, and $f_0(1370)\times$ $f_0(1710)$ for χ_{c0}. We considered $f_2(1270)\pi^0\pi^0$ for χ_{c1} and $f_2(1270)f_2(1270)$ and $f_0(1370)f_0(1710)$ for χ_{c2}. We find there is no large efficiency difference from that of phase space. The largest difference with respect to the efficiency obtained for the simulation without intermediate resonances is observed for $\chi_{c0} \to f_0(1370)f_0(1710)$ decay. We take this difference as a conservative estimate of the uncertainty due to the MC decay model and assign an uncertainty of 6.3% for the χ_{c0}, χ_{c1}, and χ_{c2} branching fractions.

(d) Fitting procedure—The χ_{cJ} yields determined from the fit to the E^*_γ spectrum determines the branching fractions. We repeat the fit with appropriate modifications to estimate the systematic uncertainties due to the fitting procedure. The difference of the derived branching fractions with respect to the values derived from the standard fit is considered as a systematic uncertainty.

We smear the resolution function of the χ_{cJ} signals obtained from MC simulations by 1% to estimate the systematic uncertainties of modeling the photon resolution in the MC simulation and shift the signal mean values by ± 1 MeV to estimate the systematic uncertainties due to the absolute energy calibration. The assigned uncertainties are given in Table III. To estimate the uncertainty due to the nonpeaking background parametrization we use a third order instead of a second order Chebychev polynomial. This uncertainty is found to be 1%. For the nominal fit, the E^*_γ spectrum is fitted in the interval 0.05–0.5 GeV. A series of fits using different E^*_γ intervals is performed and the largest change of the individual branching fractions is assigned as a systematic uncertainty (see Table III).

(e) Peaking background subtraction—The number of peaking background events is estimated from MC simulations and is subtracted from the signal yields obtained from the nominal fit. The major source of peaking background is the decay $\chi_{c1} \to \eta\pi^0\pi^0$. To determine the number of background events, the branching fraction of this decay mode is computed from the $\chi_{c1} \to \eta\pi^+\pi^-$ branching fraction exploiting the isospin relation of the two decays. The uncertainty of the branching fraction of $\chi_{c1} \to \eta\pi^0\pi^0$ leads to a systematic uncertainty of 0.8% for χ_{c1}. For χ_{c0} and χ_{c2} we take the number of subtracted background events as systematic uncertainties.

(f) Other systematic uncertainties—For the normalization of the branching fractions, the number of ψ' events in the data sample determined according to the method as given in [8] is used. This method yields a systematic uncertainty of 4%. The uncertainty due to the branching fractions $\psi' \to \gamma\chi_{cJ}$ is 3.2% for χ_{c0}, 4.3% for χ_{c1}, and 4.0% for χ_{c2}.

A systematic uncertainty of 0.5% is assigned due to the statistical error of the efficiencies as determined from MC simulations.

The systematic uncertainty due to the simulation of the trigger efficiency is found to be less than 0.1% [9].

(g) Total systematic uncertainty—We assume that all systematic uncertainties given above are independent and add them in quadrature to obtain the total systematic uncertainty.

VII. CONCLUSION

In summary we have measured the branching fractions of $\chi_{cJ} \to \pi^0\pi^0\pi^0\pi^0$ decays $\mathcal{B}(\chi_{c0} \to \pi^0\pi^0\pi^0\pi^0) = (3.34 \pm 0.06 \pm 0.44) \times 10^{-3}$, $\mathcal{B}(\chi_{c1} \to \pi^0\pi^0\pi^0\pi^0) = (0.57 \pm 0.03 \pm 0.08) \times 10^{-3}$, $\mathcal{B}(\chi_{c2} \to \pi^0\pi^0\pi^0\pi^0) = (1.21 \pm 0.05 \pm 0.16) \times 10^{-3}$ for the first time, where the quoted uncertainties are statistical and systematical, respectively. The $\pi^0\pi^0\pi^0\pi^0$ hadronic final state contains a rich substructure of intermediate resonances. The reported

branching fractions include decay modes with intermediate resonances except $\chi_{c0} \to K_S^0 K_S^0$ and $\chi_{c2} \to K_S^0 K_S^0$, which have been removed from this measurement. Our observation improves the existing knowledge of the χ_{cJ} states and provides further insight into their decay mechanisms. Based on our results detailed studies of the subresonant decay structure with increased data samples may follow in the future.

[1] G. T. Bodwin, E. Braaten, and G. P. Lepage, Phys. Rev. D **51**, 1125 (1995); H.-W. Huang and K.-T. Chao, Phys. Rev. D **54**, 6850 (1996); A. Petrelli, Phys. Lett. B **380**, 159 (1996); J. Bolz, P. Kroll, and G. A. Schuler, Eur. Phys. J. C **2**, 705 (1998); S. H. M. Wong, Eur. Phys. J. C **14**, 643 (2000).

[2] K. Nakamura *et al.* (Particle Data Group), J. Phys. G **37**, 075021 (2010).

[3] M. Ablikim *et al.* (BESIII Collaboration), Nucl. Instrum. Methods Phys. Res., Sect. A **614**, 345 (2010).

[4] J. Z. Bai *et al.* (BES Collaboration), Nucl. Instrum. Methods Phys. Res., Sect. A **344**, 319 (1994); **458**, 627 (2001).

[5] S. Agostinelli *et al.* (GEANT4 Collaboration), Nucl. Instrum. Methods Phys. Res., Sect. A **506**, 250 (2003).

[6] S. Jadach, B. F. L. Ward, and Z. Was, Comput. Phys. Commun. **130**, 260 (2000); Phys. Rev. D **63**, 113009 (2001).

[7] D. J. Lange *et al.*, Nucl. Instrum. Methods Phys. Res., Sect. A **462**, 152 (2001).

[8] M. Ablikim *et al.* (BESIII Collaboration), Phys. Rev. D **81**, 052005 (2010).

[9] N. Berger, K. Zhu *et al.*, Chinese Phys. C **34**, 1779 (2010).